



## Minimal electronic models for superconducting BiS<sub>2</sub> layers

Hidetomo Usui, Katsuhiko Suzuki, and Kazuhiko Kuroki

*Department of Engineering Science, The University of Electro-Communications, Chofu, Tokyo 182-8585, Japan*

(Received 24 July 2012; revised manuscript received 19 November 2012; published 3 December 2012)

We construct minimal electronic models for a newly discovered superconductor LaO<sub>1-x</sub>F<sub>x</sub>BiS<sub>2</sub> ( $T_c = 10.6$  K) possessing BiS<sub>2</sub> layers based on a first-principles band calculation. First, we obtain a model consisting of two Bi  $6p$  and two S  $3p$  orbitals, which give nearly electron-hole symmetric bands. Further focusing on the bands that intersect the Fermi level, we obtain a model with two  $p$  orbitals. The two bands (per BiS<sub>2</sub> layer) have a quasi-one-dimensional character with a double minimum dispersion, which gives good nesting of the Fermi surface. At around  $x \sim 0.5$  the topology of the Fermi surface changes, so that the density of states at the Fermi level becomes large. Possible pairing states are discussed.

DOI: [10.1103/PhysRevB.86.220501](https://doi.org/10.1103/PhysRevB.86.220501)

PACS number(s): 74.25.Jb, 74.20.Pq, 74.62.Bf

For the past several decades, superconductors with layered lattice structures such as cuprates,<sup>1</sup> organic conductors,<sup>2</sup> MgB<sub>2</sub>,<sup>3</sup> Sr<sub>2</sub>RuO<sub>4</sub>,<sup>4</sup> Na<sub>x</sub>CoO<sub>2</sub>,<sup>5</sup> (Hf,Zr)NCl,<sup>6</sup> and iron pnictides<sup>7</sup> have attracted much attention. These layered superconductors have been of interest in many aspects such as high  $T_c$  and/or unconventional pairing mechanisms. Quite recently, Mizuguchi *et al.* have discovered superconducting materials that possess BiS<sub>2</sub> layers, where the Bi and S atoms are aligned alternatively on a square lattice. The materials found so far are Bi<sub>4</sub>O<sub>4</sub>S<sub>3</sub>,<sup>8</sup> LaO<sub>1-x</sub>F<sub>x</sub>BiS<sub>2</sub>,<sup>9</sup> and NdO<sub>1-x</sub>F<sub>x</sub>BiS<sub>2</sub>,<sup>10</sup> which have  $T_c$  of 8.6, 10.6, and 5.6 K, respectively. Figure 1 shows the lattice structure of LaOBiS<sub>2</sub>, where partial replacement of O by F ( $x = 0.5$ ) provides electron doping and gives rise to superconductivity. These findings strongly suggest that materials with BiS<sub>2</sub> layers provide yet another family of layered superconductors exhibiting double-digit  $T_c$ , and it is of special importance to understand the underlying electronic structure of these materials.

Recent studies have shown that effective models constructed from a first-principles band calculation can provide a solid basis for the study of the mechanism of superconductivity, especially for materials with complicated band structures such as iron pnictides.<sup>11</sup> In this Rapid Communication, we perform a first-principles band calculation of LaOBiS<sub>2</sub>, from which we construct maximally localized Wannier orbitals to obtain the effective tight-binding models, i.e., the kinetic energy part of the effective Hamiltonian. The models consist of two or four bands that have a quasi-one-dimensional character, which are hybridized to give a two-dimensional Fermi surface. At around  $x \sim 0.5$  the topology of the Fermi surface changes, so that the density of states at the Fermi level becomes large. We show that the quasi-one-dimensional nature results in a nesting of the Fermi surface, which gives rise to enhanced irreducible susceptibility along the diagonals that intersects the wave vectors (0,0) and ( $\pi,\pi$ ). We discuss possible superconducting states.

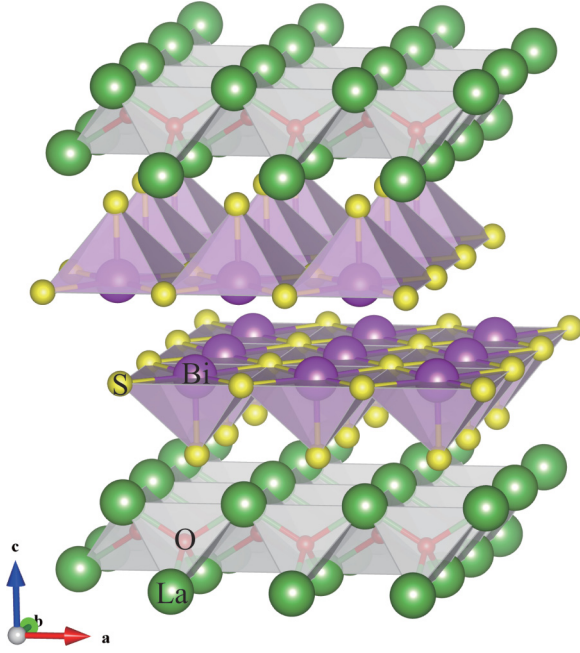
The band calculation of the mother compound LaOBiS<sub>2</sub> is performed using the WIEN2K package<sup>12</sup> and adopting the lattice structure given in Ref. 13 (see the Supplemental Material for details<sup>14</sup>). Here we present results without the spin-orbit coupling, although this coupling does have some effect on the band structure. The calculation result is shown in Fig. 2. The conduction bands around the Fermi level consists mainly of in-plane Bi  $6p$  orbital character, mixed with in-plane S  $3p$ .

From this band calculation, we obtain maximally localized Wannier orbitals,<sup>15,16</sup> which enable us to construct tight-binding models that correctly reproduce the original first-principles band structure around the Fermi level. First, we construct a 24 orbital model, which consists of six Bi  $6p$ , 12 S  $3p$ , and six O  $2p$  orbitals. The band structure of the obtained tight-binding model is shown in Fig. 3(a). Here, the thickness of the lines represent the weight of the in-plane  $p$  orbitals within the BiS<sub>2</sub> layers. Since the BiS<sub>2</sub> layers are without doubt the origin of the superconductivity, we can further obtain a model that omits the O  $2p$  orbitals, the  $3p$  orbitals of the out-of-plane S, and also the  $p_z$  orbital of the in-plane S (whose bands lie away from the Fermi level), and we are left with an eight orbital model (band not shown—see the Supplemental Material<sup>14</sup>). There are eight orbitals because there are two BiS<sub>2</sub> layers per unit cell, and each Bi and in-plane S has two  $p$  orbitals. Note that we should extract the portion of the bands that is relevant to the BiS<sub>2</sub> layers since the many-body interactions (which should be included in the forthcoming studies) take place mainly within this layer. By further neglecting the small interlayer coupling between the neighboring BiS<sub>2</sub> layers, we end up with a two-dimensional “ $p$ - $p$ ” four orbital model consisting of two Bi  $6p$  and two S  $3p$  orbitals. The band structure of this model is shown in Fig. 3(b). We write the model Hamiltonian in the form

$$H_0 = \sum_{ij} \sum_{\mu\nu} \sum_{\sigma} [t(x_i - x_j, y_i - y_j; \mu, \nu) c_{i\mu\sigma}^{\dagger} c_{j\nu\sigma} + t(x_j - x_i, y_j - y_i; \nu, \mu) c_{j\nu\sigma}^{\dagger} c_{i\mu\sigma}] + \sum_{i\mu\sigma} \varepsilon_{\mu} n_{i\mu\sigma}, \quad (1)$$

where  $c_{i\mu\sigma}^{\dagger}$  creates an electron with spin  $\sigma$  on the  $\mu$ th orbital in the  $i$ th unit cell, and  $n_{i\mu\sigma} = c_{i\mu\sigma}^{\dagger} c_{i\mu\sigma}$ . Then, the parameters of this four orbital model is given in Table I. The two  $p$  orbitals are denoted as  $p_X$  and  $p_Y$ , where the  $X$ - $Y$  axis is rotated by 45° from the  $x$ - $y$  axes [a figure of the four orbital model is not presented, but see Fig. 4(a) for the  $X$  and  $Y$  axes]. It is interesting to note that the upper and the lower bands are roughly symmetric with respect to the gap.

An even more simple model is the one which focuses only on the bands that intersect the Fermi level. By extracting these bands using the maximally localized Wannier orbitals centered at the Bi sites and neglecting the interlayer hoppings, the


 FIG. 1. (Color online) The lattice structure of LaOBiS<sub>2</sub>.

Hamiltonian reduces to a two-dimensional two orbital model [Fig. 4(a)], whose band structure is shown in Fig. 4(b) and the hopping parameters given in Table II. Assuming a rigid band, the Fermi surface for this model is obtained in Fig. 4(c) for two doping ratios,  $\delta = 0.25$  and  $0.5$ . Here  $\delta$  is defined as the number of doped electrons per Bi site, and satisfies  $\delta = x$  in an ideal situation. At around  $\delta \sim 0.5$  the topology of the Fermi surface changes, so that the density of states at the Fermi level becomes large around this band filling. The  $p_X$  and  $p_Y$  bands have essentially a one-dimensional character, where the main hopping integrals ( $t'$ ) exist between next nearest neighbor sites,

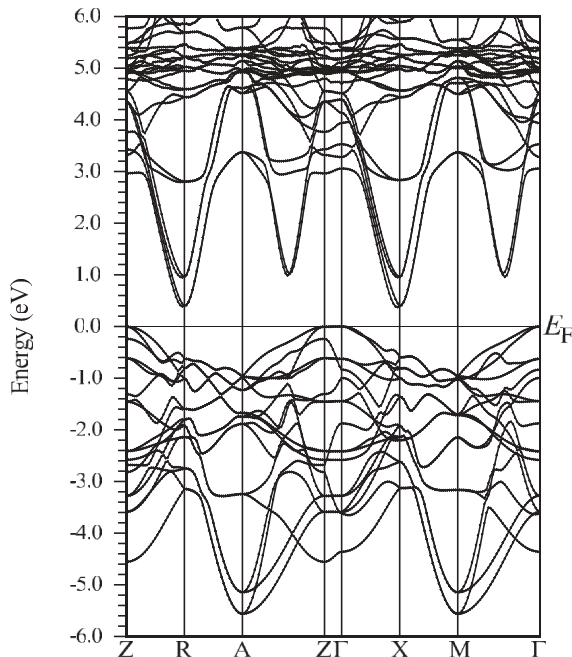
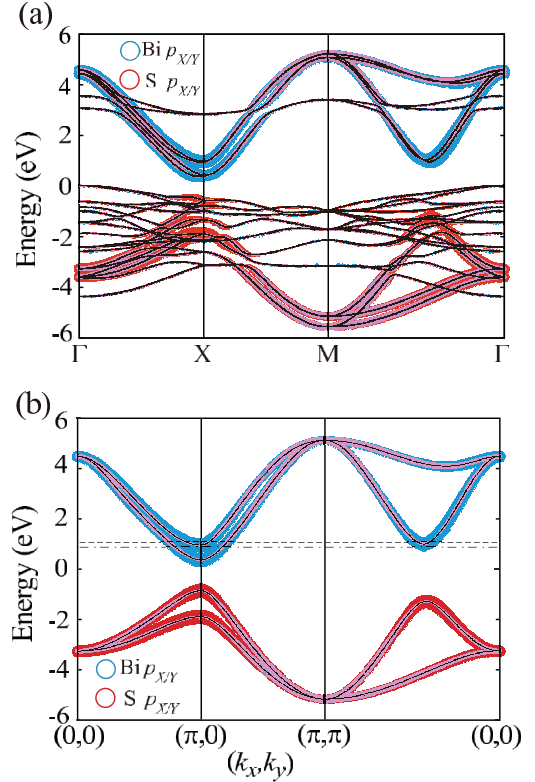


FIG. 2. The first-principles band structure is shown.


 FIG. 3. (Color online) (a) The 24 orbital model and (b) the four orbital model. In (b), the dashed (dotted-dashed) lines denote the Fermi energy for the doping ratio  $\delta = 0.5$  ( $\delta = 0.25$ ).

as shown in Fig. 4(a) and Table II. Thus the one-dimensional bands essentially have the forms

$$\varepsilon_X(k) = 2t' \cos(k_x + k_y), \quad \varepsilon_Y(k) = 2t' \cos(k_x - k_y), \quad (2)$$

which have a double well band dispersion along  $(k_x, k_y) = (-\pi, -\pi) \rightarrow (0, 0) \rightarrow (+\pi, +\pi)$  or  $(-\pi, +\pi) \rightarrow (0, 0) \rightarrow (+\pi, -\pi)$ , as shown in Fig. 4(d). The intraorbital ( $t$ ) as well

TABLE I. Hopping parameters  $t(\Delta x, \Delta y; \mu, \nu)$  or the on-site energies  $\varepsilon_\mu$  for the four orbital model. The orbitals  $\mu = 1, 2, 3, 4$  correspond to Bi  $p_Y, p_X, S p_Y, p_X$  orbitals, respectively. We follow the notations in Ref. 11, i.e.,  $I$ , and  $\sigma_d$  correspond to  $t(-\Delta x, -\Delta y; \mu, \nu)$ ,  $t(\Delta y, \Delta x; \mu, \nu)$ , respectively, where “ $\pm$ ” means that the corresponding hopping is equal to  $\pm t(\Delta x, \Delta y; \mu, \nu)$ , respectively.

$(\mu, \nu)$	$[\Delta x, \Delta y]$					$I$	$\sigma_d$
	$[0, 0]$	$[1, 0]$	$[-1, 0]$	$[1, -1]$	$[1, 1]$		
(1, 1)	0.890	0.223	0.223	0.103	0.082	+	+
(1, 2)		0.100	0.100			+	-
(1, 3)	0.486		-2.034			+	+
(1, 4)						+	+
(2, 2)	0.890	0.223	0.223	0.082	0.103	+	+
(2, 3)						+	+
(2, 4)	2.034		-0.486			+	+
(3, 3)	-1.113	-0.110	-0.110	0.100	0.023	+	+
(3, 4)		0.154	0.154			+	-
(4, 4)	-1.113	-0.110	-0.110	0.023	0.100	+	+

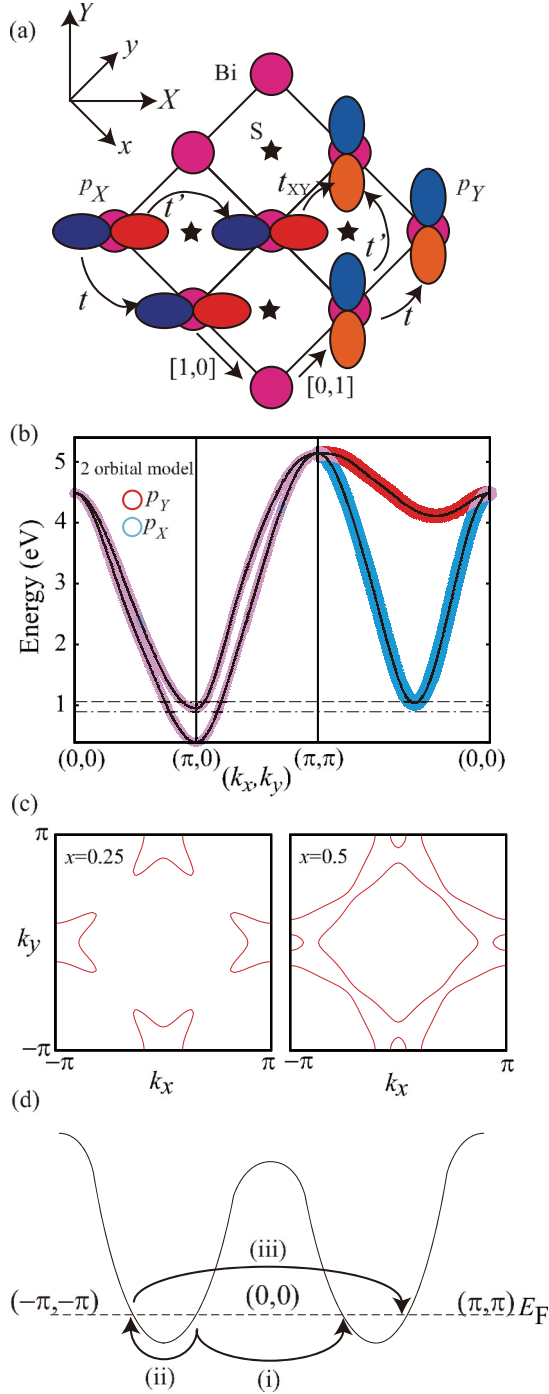


FIG. 4. (Color online) (a) The tight-binding model on the Bi square lattice is shown along with the hoppings of  $p_X$  and  $p_Y$  orbitals. The stars denote the position of the S atom, whose  $p$  orbitals are explicitly considered in the four orbital model, but are integrated out in the two orbital model. (b) The band structure of the two orbital model. The dashed (dotted-dashed) lines denote the Fermi energy for the doping ratio  $\delta = 0.5$  ( $\delta = 0.25$ ). (c) The Fermi surface of the two orbital model for the doping rate of  $\delta = 0.25$  and  $\delta = 0.5$ . (d) A schematic figure of the  $p_X$  band along  $(-\pi, -\pi) \rightarrow (0,0) \rightarrow (+\pi, +\pi)$ . Three types of nesting vectors are shown by the arrows.

as the interorbital ( $t_{XY}$ ) nearest neighbor hoppings give the two dimensionality of the system.

TABLE II. Hopping parameters and on-site energies for the two orbital model.  $\mu = 1, 2$  correspond to  $p_Y, p_X$ , respectively. Here  $t' = 0.880$ ,  $t = -0.167$ , and  $t_{XY} = 0.107$ .

$(\mu, \nu)$	$[\Delta x, \Delta y]$						$I$	$\sigma_d$	
	$[0,0]$	$[1,0]$	$[1,-1]$	$[1,1]$	$[2,0]$	$[2,1]$			$[2,-1]$
(1,1)	2.811	-0.167	0.880	0.094		0.014	0.069	+	+
(1,2)		0.107			-0.028	0.020	0.020	+	-
(2,1)		0.107			-0.028	0.020	0.020	+	-
(2,2)	2.811	-0.167	0.094	0.880		0.069	0.014	+	+

The one-dimensional nature of the bands provides good nesting of the Fermi surface. To see this effect, we calculate for the two orbital model the  $4 \times 4$  irreducible susceptibility matrix in the orbital representation,  $\chi_{l_1, l_2, l_3, l_4}^0(\mathbf{q}) = \sum_{\mathbf{k}} G_{l_1, l_3}^0 G_{l_4, l_2}^0$ , where  $G^0$  is the  $2 \times 2$  bare Green's function matrix. In Fig. 5, we show the largest eigenvalue of the irreducible susceptibility matrix for the doping ratio of  $\delta = 0.25$  and  $0.5$ . The diagonal structures that go through  $(0,0)$  or  $(\pi, \pi)$  are due to the nesting shown by the arrows in Fig. 4(d). Note that if the nearest neighbor hoppings do not exist and the bands have the form in Eq. (2), the nestings (i)–(iii) are equivalent, while this equivalence is lost in the presence of  $t$  (and additional hoppings).

Finally, let us discuss the possible pairing states and the superconducting gap structure. Since the many-body term of the effective Hamiltonian is not determined here, there are several possibilities at present. The most relevant bands have mainly a  $6p$  character, which gives a wide spread of the Wannier orbitals, so that the electron-electron interactions may not be very strong and short ranged as in the  $3d$ -orbital-based materials such as the cuprates and iron-based superconductors. In that case, the electron-phonon interaction can be playing the main role in the Cooper pairing, and the good nesting of the Fermi surface may cooperate to give an enhanced attractive pairing interaction around the nesting vectors. This can give rise to an  $s$ -wave pairing with a constant gap sign as shown in Fig. 6(a). It is interesting to point out that Bi-based superconductors  $(\text{Ba}, \text{K})(\text{Bi}, \text{P})\text{O}_3$  (Refs. 17 and 18) are also known to have Fermi surface nesting, but with a  $O-2p$  and  $\text{Bi}-6s$  orbital character,<sup>19</sup> which is different from the present material. A more exotic possibility for the same type of gap is

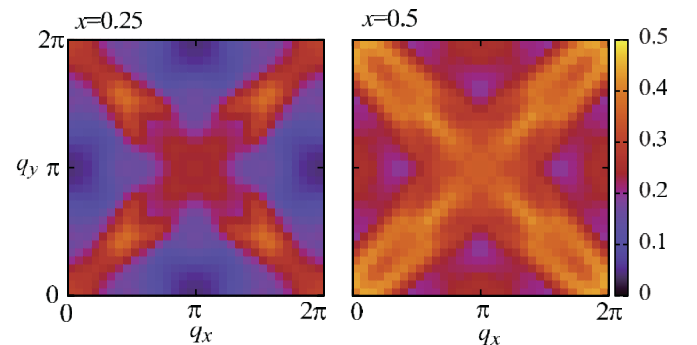


FIG. 5. (Color online) The largest eigenvalue of the irreducible susceptibility matrix for  $\delta = 0.25$  and  $0.5$ .

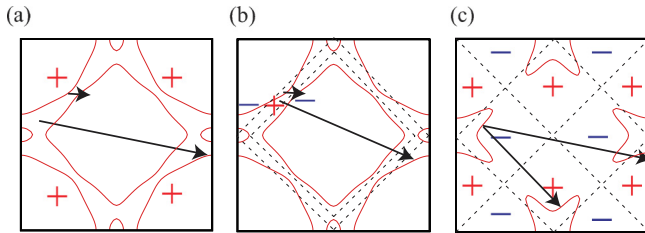


FIG. 6. (Color online) (a) Sign conserving  $s$  wave for attractive pairing interactions such as mediated by phonons or charge fluctuations, (b) sign reversing  $s$  wave, and (c)  $d$ -wave superconducting gaps obtained for repulsive pairing interactions mediated by spin fluctuations.

related to the fact that the system is close to a band insulator, where electron-hole excitations might be playing an important role in the pairing.<sup>20</sup> In fact, if we consider electron-electron interactions in the four orbital model, the system can be viewed as two interacting charge-transfer-type insulating bands. This is similar to the situation studied in Ref. 21, where the occurrence of superconductivity was proposed for systems with a metallic band interacting with a charge-transfer-type insulating band. In this context, it should be noted that the analysis for the Bi  $6p$ -S  $3p$  four orbital model can give different results from those for the two orbital model regarding the superconducting state, because the band filling is different, i.e., the four orbital model is a nearly half-filled, electron-hole symmetric system, while the two orbital model has a small band filling.

On the other hand, if we assume a short-ranged repulsive interaction, the present two orbital model provides a fundamental problem of the pairing state in repulsively interacting quasi-one-dimensional systems, apart from its relevance to the BiS<sub>2</sub> layers. Namely, the occurrence of superconductivity in repulsively interacting one-dimensional systems with a double-well-type band structure was studied in the late 1990's, where interaction (ii) in Fig. 4(d) dominates for a certain parameter regime to give a gap that reverses its sign between the inner and the outer Fermi points.<sup>22–25</sup> The existence of  $t$  in Fig. 4(a) is essential in this case, because this makes the interactions (i)/(iii) and (ii) inequivalent. In fact, by adding on-site intraorbital ( $U$ ) and interorbital interactions ( $U' = 2U/3$  and the Hund's coupling and the pair hoppings  $J = J' = U/6$ ), and applying a multiorbital random phase approximation<sup>26,27</sup> to obtain the spin-fluctuation-mediated pairing interaction, we find the sign reversing  $s$ -wave gap shown in Fig. 6(b) for

large doping (e.g.,  $\delta = 0.5$  and  $U = 1.8$  eV) and the  $d$ -wave superconducting gap shown in Fig. 6(c) for small doping (e.g.,  $\delta = 0.25$  and  $U = 2.43$  eV).

These gaps are determined by cooperation or competition between the repulsive (sign reversing) spin-singlet pairing interactions driven by the nestings given in Fig. 4(d). The gap in Fig. 6(b) indeed exhibits a sign reversal between the inner and the outer Fermi surfaces. On the other hand, the gap in Fig. 6(c) is obtained by reversing the gap sign for both interactions (i) and (ii). To make the gap have even parity requires additional nodes at  $k_x = \pm k_y$ . The reason why this  $d$  wave is favored for small doping is because the diagonal nodes do not intersect the Fermi surface in this situation. In an ideal situation, the gaps in Figs. 6(a) and 6(b) [6(c)] can be distinguished by  $T_1^{-1}$  measurement in the nuclear magnetic resonance (NMR) experiments. For the gap in Fig. 6(a),  $T_1^{-1}$  should exhibit a coherence peak followed by a steep decrease, while for Fig. 6(b) [Fig. 6(c)] the coherence peak should be (nearly) absent. It is more difficult to distinguish the gaps in Figs. 6(b) and 6(c) because even for the  $d$ -wave case in Fig. 6(c), the nodes intersecting the Fermi surface are accidental. Therefore, other phase sensitive experiments are necessary.

Finally, yet another possibility related to the quasi-one-dimensionality is the spin-triplet pairing. In fact, the present band structure also has a similarity with the quasi-one-dimensional bands (the hybridized  $d_{xz/yz}$  bands) in Sr<sub>2</sub>RuO<sub>4</sub>, where some theoretical studies have suggested the possibility of spin-triplet pairing originating from these bands.<sup>28–31</sup> NMR experiments will also provide a test for this possibility.

To summarize, we have obtained effective tight-binding models for the superconducting BiS<sub>2</sub> layers by performing a band calculation for LaOBiS<sub>2</sub> and exploiting the maximally localized Wannier orbitals. The model consists of  $p_X$  and  $p_Y$  orbitals, and the dominant next nearest neighbor hoppings lead to quasi-one-dimensional bands, which give nesting of the Fermi surface. Considering the quasi-one-dimensional as well as the doped-band-insulator nature of the band structure, there are several interesting possibilities for the superconducting state depending on the dominating many-body interactions.

We are grateful to Y. Mizuguchi for showing us the experimental results for LaO<sub>1-x</sub>F<sub>x</sub>BiS<sub>2</sub> prior to publication. We also acknowledge all the collaborators in Ref. 8. This study has been supported by Grants-in-Aid for Scientific Research from MEXT of Japan and from the Japan Society for the Promotion of Science.

<sup>1</sup>J. G. Bednorz and K. A. Müller, *Z. Phys. B: Condens. Matter* **64**, 189 (1986).

<sup>2</sup>For a recent review, see A. Ardavan *et al.*, *J. Phys. Soc. Jpn.* **81**, 011004 (2012).

<sup>3</sup>J. Nagamatsu *et al.*, *Nature (London)* **410**, 63 (2001).

<sup>4</sup>Y. Maeno *et al.*, *Nature (London)* **372**, 532 (1994).

<sup>5</sup>K. Takada *et al.*, *Nature (London)* **422**, 53 (2003).

<sup>6</sup>S. Yamanaka, K. Hotehama, and H. Kawaji, *Nature (London)* **392**, 580 (1998).

<sup>7</sup>Y. Kamihara *et al.*, *J. Am. Chem. Soc.* **130**, 3296 (2008).

<sup>8</sup>Y. Mizuguchi *et al.*, arXiv:1207.3145 [Phys. Rev. B (to be published)].

<sup>9</sup>Y. Mizuguchi *et al.*, *J. Phys. Soc. Jpn.* **81**, 114725 (2012).

<sup>10</sup>S. Demura *et al.*, arXiv:1207.5248.

<sup>11</sup>K. Kuroki, S. Onari, R. Arita, H. Usui, Y. Tanaka, H. Kontani, and H. Aoki, *Phys. Rev. Lett.* **101**, 087004 (2008).

<sup>12</sup>P. Blaha, K. Schwarz, G. K. H. Madsen, D. Kvasnicka, and J. Luitz, *Wien2k: An Augmented Plane Wave + Local Orbitals Program for Calculating Crystal Properties* (Vienna University of Technology, Wien, 2001).

- <sup>13</sup>V. S. Tanryverdiev and O. M. Aliev, *Inorg. Mater.* **31**, 1361 (1995).
- <sup>14</sup>See Supplemental Material at <http://link.aps.org/supplemental/10.1103/PhysRevB.86.220501> for details of the first-principles calculation and the model construction.
- <sup>15</sup>N. Marzari and D. Vanderbilt, *Phys. Rev. B* **56**, 12847 (1997); I. Souza, N. Marzari, and D. Vanderbilt, *ibid.* **65**, 035109 (2001); The Wannier functions are generated by the code developed by A. A. Mostofi, J. R. Yates, N. Marzari, I. Souza, and D. Vanderbilt, <http://www.wannier.org/>.
- <sup>16</sup>J. Kunes, R. Arita, P. Wissgott, A. Toschi, H. Ikeda, and K. Held, *Comput. Phys. Commun.* **181**, 1888 (2010).
- <sup>17</sup>A. W. Sleight *et al.*, *Solid State Commun.* **17**, 27 (1975).
- <sup>18</sup>L. F. Mattheiss, E. M. Gyorgy, and D. W. Johnson, *Phys. Rev. B* **37**, 3745 (1988).
- <sup>19</sup>L. F. Mattheiss and D. R. Hamann, *Phys. Rev. B* **28**, 4227 (1983).
- <sup>20</sup>W. A. Little, *Phys. Rev.* **134**, A1416 (1964).
- <sup>21</sup>K. Kuroki and H. Aoki, *Phys. Rev. B* **48**, 7598 (1993).
- <sup>22</sup>M. Fabrizio, *Phys. Rev. B* **54**, 10054 (1996).
- <sup>23</sup>K. Kuroki, R. Arita, and H. Aoki, *J. Phys. Soc. Jpn.* **66**, 3371 (1997).
- <sup>24</sup>K. Sano *et al.*, *J. Phys. Soc. Jpn.* **74**, 2885 (2005).
- <sup>25</sup>T. Nakano, K. Kuroki, and S. Onari, *Phys. Rev. B* **76**, 014515 (2007).
- <sup>26</sup>T. Takimoto, T. Hotta, and K. Ueda, *Phys. Rev. B* **69**, 104504 (2004).
- <sup>27</sup>K. Yada and H. Kontani, *J. Phys. Soc. Jpn.* **74**, 2161 (2005).
- <sup>28</sup>T. Kuwabara and M. Ogata, *Phys. Rev. Lett.* **85**, 4586 (2000).
- <sup>29</sup>M. Sato and M. Kohmoto, *J. Phys. Soc. Jpn.* **69**, 3505 (2000).
- <sup>30</sup>K. Kuroki, M. Ogata, R. Arita, and H. Aoki, *Phys. Rev. B* **63**, 060506(R) (2001).
- <sup>31</sup>T. Takimoto, *Phys. Rev. B* **62**, 14641(R) (2000).